Validation of reduced transport models for integrated modeling of AUG L-mode discharges in the European Transport Simulator

B. Brandström[1], D. Yadykin[1], P. Strand[1], D.Coster[2], M. M. Skyllas[1], the ASDEX Upgrade Team[2,a]

[1]Department of Physics and Astronomy, Chalmers University of Technology, SE-412 96 Gothenburg, Sweden

[2] Max-Planck-Institut für Plasmaphysik, Boltzmannstrasse 2, D-85748

[a]See author list of T. Pütterich et al, Nucl. Fusion **66** 116002 (2026) https://doi.org/10.1088/1741-4326/ae61c8

1 Introduction

For the development of operating scenarios for future tokamaks, like ITER, it is essential that anomalous plasma transport can be efficiently and accurately modeled. Such modeling capabilities must be available for the full plasma radius and all phases of a discharge, including ramp-up and ramp-down. In this work, we assess the ability of three reduced transport models: (i) the semi-empirical Bohm-gyroBohm (BgB) model [1], (ii) the EDWM model [2] and (iii) TGLF-SAT2 [3, 4] with electrostatic settings, to simulate temperature and density profiles from the flat top phase of two ASDEX Upgrade (AUG) L-mode plasmas. Of (i)-(iii), TGLF-SAT2 is expected to be the most accurate; recent work indicate that it can be used in integrated modeling to reproduce the dependency of stored energy on engineering parameters seen in scaling laws [5], and to successfully predict kinetic profiles in L-mode tokamak plasmas [6]. Simulations in this work have been performed with the European Transport Simulator (ETS) [7], an integrated modeling framework which couples multiple physics models to make predictions and interpretations of kinetic plasma profiles in tokamak experiments.

2 Modeling set up and experimental data

The ETS PAF (Persistant Actor Framework) [8] workflow, built on the multi-scale coupling framework MUSCLE3 [9], was used to predict flat-top steady state T_i, T_e and n_i profiles (n_e was determined from quasi-neutrality) from the AUG L-mode discharges AUG#35475 (D) and AUG#35221 (H) (previously modeled with ASTRA+TGLF-SAT2 in Ref. [5]). Predictions were made for $0.0 \leq \rho \leq 1.0$, where ρ is the normalized toroidal flux label coordinate. Experimental data and engineering parameters treated in TRVIEW [10] were initial- and boundary conditions for the simulations. Current density and equilibrium were prescribed from ETS interpretations of the experimental data, where q-profiles had relaxed so that $|q(\rho = 0)| \simeq 1$.

AUG#35475 and AUG#35221 had similar engineering parameters: $B_T \sim 2.45$ T, $I_p = 0.83$ MA, $\langle n_e \rangle_{\text{line}} \sim 2 \cdot 10^{19} \text{m}^{-3}$. Three consecutive heating mixes were applied to the flat-top phase of both discharges: 100% NBI, ∼50%/50% NBI and EC, and 100% EC. Total power was ~ 1.3 MW for all time points considered. Time points modeled for AUG#35475 (AUG#35221) were: NBI heating $t = 2.97$ (2.75) s, mixed heating $t = 4.5$ (4.45) s and EC heating $t = 5.47$ (5.35) s. Auxiliary heating in ETS was modeled with RABBIT [11](NBI heating and fast particles) and TORBEAM [12] (EC heating), neoclassical transport with NCLASS [13]. Fueling was modeled with a Gaussian particle source (centered around $\rho = 1$) of the fully ionized main species. The source width was fit to a BgB simulation of the AUG#35475 NBI heated phase ($t = 2.97$ s), and the number of particles from the source was scaled to a target $\langle n_e \rangle_{\text{vol}}$ (calculated from experimental data for each modeled time point). Fully ionized Carbon was included in the simulations, with static density profiles such that $Z_{\text{eff}} = 1.5$ across ρ for the initial profiles for both discharges. Carbon temperature was predicted by ETS, to allow it to equilibrate to T_i. Plasma rotation was assumed to be zero for all simulations.

3 ETS predictions and results from TGLF-SAT2 standalone $k_y\rho_s$ scans

The accuracy of the reduced transport models was evaluated via σ(d), defined as in Ref. [14]: $\sigma(d) = \sum_i^N (2/N) \left| \frac{d_{\text{exp},\rho_i} - d_{\text{ETS},\rho_i}}{d_{\text{exp},\rho_i} + d_{\text{ETS},\rho_i}} \right|$, where d_{exp,ρ_i} is the experimental data for a signal d at a position ρ_i, and d_{ETS,ρ_i} is the ETS prediction for the same signal and position. The fraction of ETS total thermal energy to experimental was also considered: $W = W_{\text{ETS}}/W_{\text{exp}}$.

Scans over $k_y\rho_s$ with standalone TGLF-SAT2 (same settings as in ETS+TGLF-SAT2 predictive runs) were also performed for a few radial points of AUG#35475 predicted steady state and initial (i.e. experimental) data, to compare unstable modes identified by TGLF-SAT2 to those found by linear GENE.

3.1 Accuracy of the transport models

Fig. 3 (NBI heating), Fig. 4 (mixed heating), and Fig. 5 (EC heating) show ETS predicted kinetic profiles, together with their experimental counterparts for AUG#35475 and AUG#35221. Resulting W and $\sigma(d) \cdot 100$ (error as a percentage) for $d = T_i$, n_i, T_e are shown in Fig. 1a (AUG#35475) and Fig. 1b (AUG#35221). The gray regions in Fig. 1 cover $W_{\text{exp}} \pm 15\%$ and +30% for σ. For all transport models, profiles from the EC heated phase proved most difficult to model accurately.

EDWM. For the NBI heated phase (green markers in Fig. 1 and green dotted profiles in Fig. 3), thermal

energy was overestimated by 40% (80%) for #35475 (#35221), and $\sigma(T_i)$ and $\sigma(T_e)$ were above 30% (40%). As EDWM predictions got more inaccurate as the fraction of EC heating was increased, predictions for plasmas with EC heating are not shown here. Instead we note that EDWM is currently not capable of modeling EC heated plasmas sufficiently well, suspected to be (in part) due to the lack of an ETG model.

BgB. The dashed blue profiles in Figs. 3, 4 indicate that BgB performs well for NBI heated plasmas, and for the NBI+EC heating mix; for the EC heated plasmas (Fig. 5), central T_i are underestimated and T_e overestimated. As shown by the blue markers in Fig. 1, $\sigma(T_e)$ and $\sigma(n_i) < 30\%$ ($< 35\%$) for AUG#35475 (AUG#35221), and thermal energy predictions are within 15% of experimental value for all three heating mixes in both discharges.

TGLF-SAT2. Temperature predictions with TGFL-SAT2 for heating mixes with NBI yield overpredictions of central T_i (dash-dotted red, Figs. 3, 4). For the purely EC heated phase (Fig. 5)—when $T_e/T_i \sim 6.2$ (4.1) at $\rho = 0$ for the experimental profiles from AUG#35475 (AUG#35221)—T_i is instead underpredicted and T_e overestimated. TGLF-SAT2 predicts flatter edge density gradients than seen in the experimental data. The red markers in Fig 1 show predicted thermal energy W_{ETS} is $\pm 15\%$ of W_{exp} for both discharges, and profile errors $\sigma(d)$ are $< 30\%$ for $d = n_i$, T_e for AUG#35475, and $\sigma(d) < 30\%$ for $d = n_i$, T_e, T_i for AUG#35221.

3.2 Comparison of standalone TGLF-SAT2 k_y scans to linear GENE

A companion work (see conference contribution by M.M. Skyllas) where linear and non-linear gyrokinetic simulations have been performed with GENE [15] on the TRVIEW treated experimental data from AUG#35475, for the three heating mixes at three radial positions ($\rho = 0.3$, $\rho = 0.6$ and $\rho = 0.9$) enabled comparison between growthrates and frequencies of unstable modes found by linear GENE, and those identified by standalone TGLF-SAT2. GENE used the TRVIEW reconstructed experimental equilibria ("exp. eq."), while the predictive ETS runs used interpreted equilibria, relaxed so that $|q(\rho = 0)| \simeq 1$ ("ETS eq."). Therefore, multiple standalone TGLF-SAT2 k_y scans were performed for each radial point, investigating the impact of different equilibria and gradients on the standalone TGLF-SAT2 results. Here, we present results from k_y-scans of the NBI heated phase ($t = 2.97$ s) of AUG#35475, at $\rho = 0.6$ and $\rho = 0.9$.

The red and black markers in Fig. 2 indicate that using the ETS eq. (hollow black) instead of the exp. eq. (red) in standalone TGLF-SAT2 (both scans used experimental gradients) removes the negative frequency mode at $k_y\rho_s > 2.5$ for $\rho = 0.6$, and shifts where in $k_y\rho_s$ the transition between negative and positive ω occurs for $\rho = 0.9$. Qualitative comparison to GENE results (blue) indicate that for $k_y\rho_s < 1.0$, both codes find modes with frequencies in the ion direction ($\omega > 0$) at $\rho = 0.6$, and modes with frequencies in the electron direction ($\omega < 0$) at $\rho = 0.9$. At higher $k_y\rho_s$, TGLF-SAT2 results diverge from GENE results, finding $\omega \leq 0$ modes for the higher k_y where GENE finds $\omega \geq 0$ modes.

The impact of the gradients on TGLF-SAT2 results is shown by the hollow black (experimental gradients, ETS eq.) and green (ETS predicted (steady state) gradients, ETS eq.) in Fig. 2. With the ETS gradients (green), a $\omega < 0$ mode is found for $k_y\rho_s > 1$ at $\rho = 0.6$, while there is no mode found for $k_y\rho_s > 0.9$ with the experimental gradients (black). At $\rho = 0.9$, the ETS gradients give values of ω that are shifted up by around 0.4 compared to what is obtained with the experimental gradients. As with the different equilibria, TGLF-SAT2 and GENE disagree at higher $k_y\rho_s$.

4 Conclusion and outlook

For the two AUG L-mode discharges considered here, ETS with BgB or TGFL-SAT2 predicted total thermal energy within 15% of experimental values for all three heating mixes, with smallest profile errors $\sigma(d)$ for mixed or NBI heating. EDWM was the least accurate model for the NBI phase, and unable to model EC heated plasmas. The accuracy EDMW improved for the D discharge compared to the H discharge, indicating that EDWM does not capture the isotope scaling.

ETS predictions for EC heated plasmas indicate that further work is needed for accurate modeling: central T_i was underestimated, while central T_e was overpredicted. ETS+TGLF-SAT2 predicted n_i gradients indicate consistent overprediction of particle transport at $\rho > 0.8$. Preliminary analysis of standalone TGLF-SAT2 and GENE k_y scans indicate that the two codes diverge on the electron scale, but qualitatively agree on the ion k_y scale with NBI heating. The discrepancies found between the two codes are in part due to differences in the gradients and the equilibria used.

Future work include more thorough sensitivity scans for standalone TGLF-SAT2 predictions with respect to equilibria, gradients, rotation, settings, etc. For predictive simulations, ETS and/or TGLF treatment of plasma rotation is expected to impact predicted transport; the effect of including the rotation in simulations is yet to be examined (expected to stabilize ITG turbulence), as we in this work assumed zero toroidal rotation.

Further improvements to/advancements of ETS might include (but are not limited to): adding analytic ETG to EDWM; add neutral transport/fueling (ongoing); adding sawtooth model. Future predictive mod-

eling with ETS is aimed at performing ramp-up simulations and core-edge coupling—the journey there will likely contain further L-mode simulations (additional AUG discharges, discharges from other machines, eg. JT-60SA), exploration of impact of impurity content, the q-profile and other engineering parameters, and continued/extended validation of reduced transport models against gyrokinetic GENE simulations.

Acknowledgments

Regarding the experimental data used in this work, the authors gratefully acknowledge the contributions from R. Fischer (profiles with the integrated data analysis suite) and R.M. McDermott (charge exchange recombination spectroscopy measurements).
This work was supported by the Swedish Energy Agency [grant number P2023-01345].
This work has been carried out within the framework of the EUROfusion Consortium, funded by the European Union via the Euratom Research and Training Programme (Grant Agreement No 101052200 — EUROfusion). Views and opinions expressed are however those of the author(s) only and do not necessarily reflect those of the European Union or the European Commission. Neither the European Union nor the European Commission can be held responsible for them.

References

[1] V.V. Parail et al. *Nucl. Fusion*, 39(3):429, 1999.

[2] P. Strand et al. In *Proceedings of the 31st EPS Conference on Plasma Physics*, pages 28G P–5.187, 2004.

[3] G. M. Staebler et al. *Phys. Plasmas*, 14(5):055909, 2007.

[4] G. M. Staebler and J. E. Kinsey. *Phys. Plasmas*, 17(12): 122309, 2010.

[5] C. Angioni et al. *Nucl. Fusion*, 62(6):066015, 2022.

[6] G.M. Staebler et al. *Nucl. Fusion*, 64(8):085002, 2024.

[7] D. P. Coster et al. *IEEE Trans. on Plasma Science*, 38: 2085–2092, 2010.

[8] D. Coster et al. In *51st EPS Conference on Plasma Physics*. European Physical Society, 2025.

[9] L. E. Veen et al. In *Computational Science – ICCS 2020*, pages 425–438, 2020.

[10] G. Tardini et al. *Nucl. Fusion*, 64(5):056014, 2024.

[11] M. Weiland et al. *Nucl. Fusion*, 58(8):082032, 2018.

[12] E. Poli et al. *Comput. Phys. Commun.*, 225:36–46, 2018.

[13] W. A. Houlberg et al. *Phys. Plasmas*, 4(9):3230–3242, 1997.

[14] M. Marin et al. *Nucl. Fusion*, 65(3):036015, 2025.

[15] F. Jenko et al. *Phys. Plasmas*, 7(5):1904–1910, 2000.

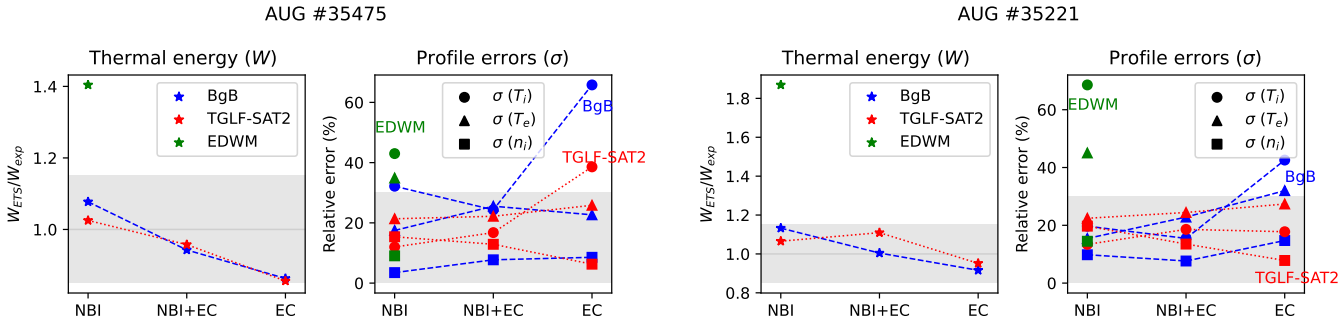

(a) AUG#35475 (D) (b) AUG#35221 (H)

Figure 1: Fraction of ETS predicted thermal energy to experimental thermal energy ($W = W_{\mathrm{ETS}}/W_{\mathrm{exp}}$), and errors $\sigma(d)$ in the predicted T_i, n_i and T_e w.r.t. experimental profiles, for both discharges at each of the three heating phases.

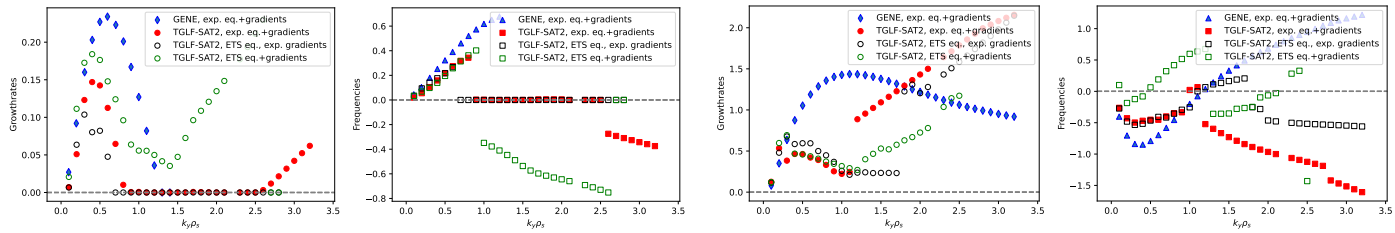

(a) NBI heating, $\rho = 0.6$ (b) NBI heating, $\rho = 0.9$

Figure 2: Effect of different equilibria and gradients on growthrates (circles) and frequencies (squares) from standalone TGLF-SAT2 k_y scans on AUG#35475 (NBI heating, $t = 2.97$ s), at two radial points. Results using experimental gradients but different equilibria are shown in red (experimental eq.) and hollow black (ETS eq.). For impact of different gradients using the ETS eq., compare hollow black (exp. gradients) and hollow green (ETS gradients) markers. GENE linear results (blue diamonds/triangles) are shown for comparison.

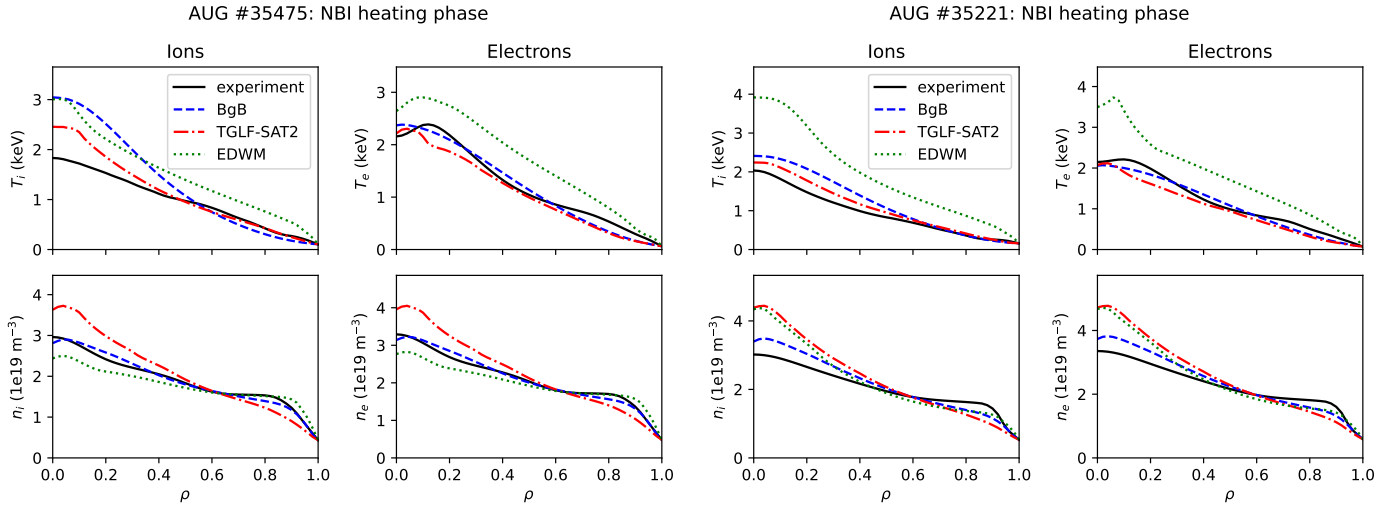

(a) AUG #35475 (D): $t = 2.97$ s. (b) AUG #35221 (H): $t = 2.75$ s.

Figure 3: ETS predicted (steady state) and experimental (solid) density and temperature profiles during the NBI heated phases of the two discharges.

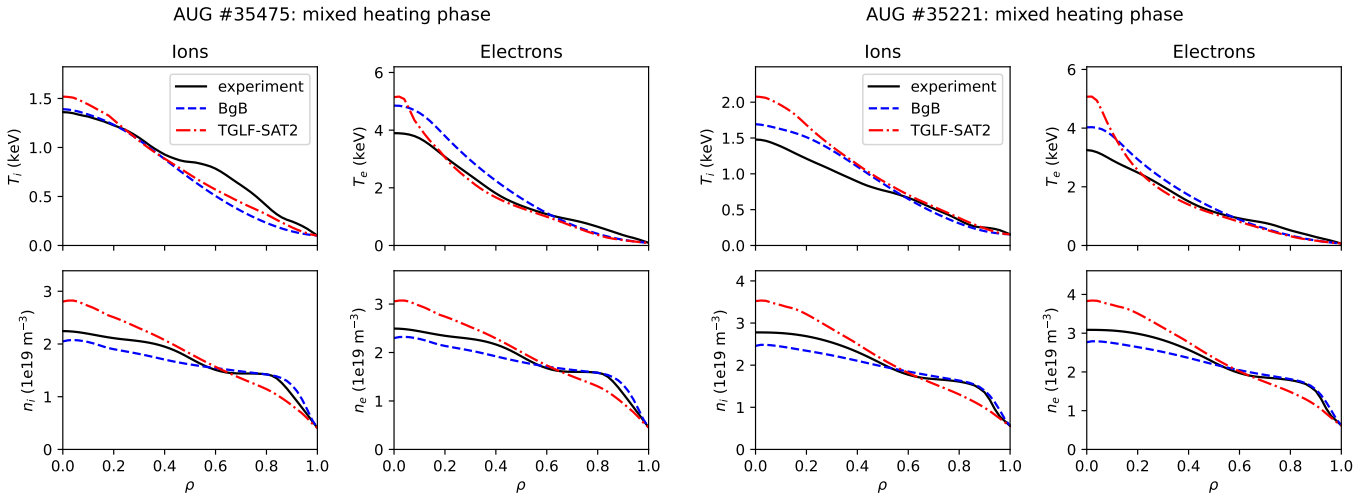

(a) AUG #35475 (D): $t = 4.5$ s. (b) AUG #35221 (H): $t = 4.45$ s.

Figure 4: ETS predicted (steady state) and experimental (solid) density and temperature profiles during the EC+NBI (mixed) heated phases of the two discharges.

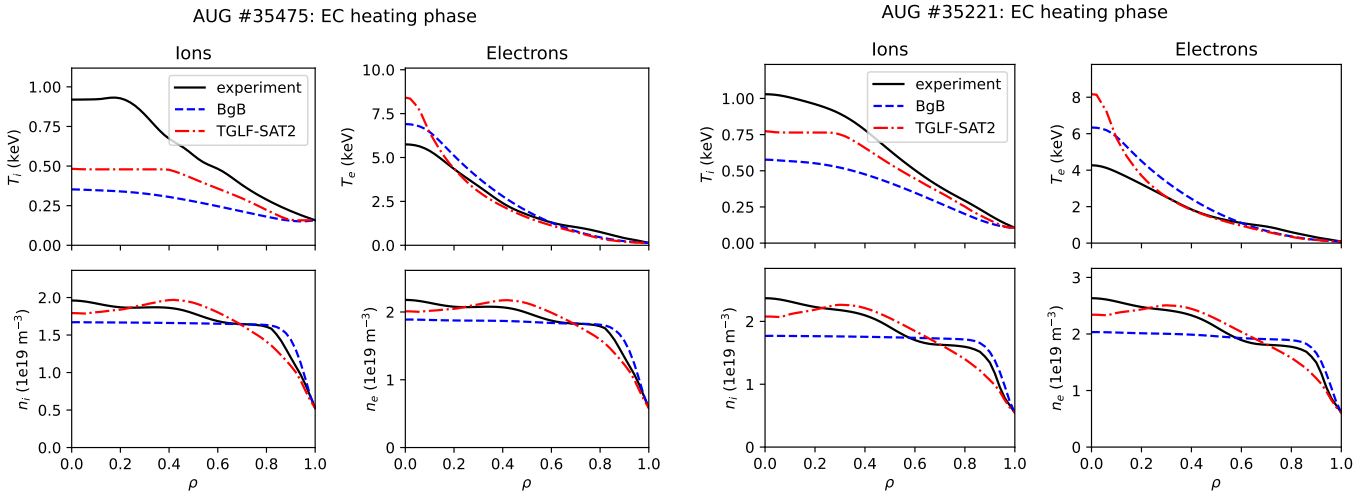

(a) AUG #35475 (D): $t = 5.46$ s. (b) AUG #35221 (H): $t = 5.35$ s.

Figure 5: ETS predicted (steady state) and experimental (solid) density and temperature profiles during the EC heated phases of the two discharges.